RSC Advances

PAPER

View Article Online
View Journal | View Issue

Cite this: *RSC Adv.*, 2023, **13**, 7102

Distribution, sources, and ecological risk assessment of polycyclic aromatic hydrocarbons in agricultural and dumpsite soils in Sierra Leone†

Mariama Janneh,[abc] Chengkai Qu,[a] Yuan Zhang,[a] Xinli Xing,[ab] Oscar Nkwazema,[d] Fatuma Nyihirani[ab] and Shihua Qi *[ab]

This study investigates the concentration and distribution of polycyclic aromatic hydrocarbons (PAHs) in soils, potential sources, risk assessment, and soil physicochemical properties influencing PAH distribution in developed and remote cities in Sierra Leone. Seventeen topsoil samples (0–20 cm) were collected and analyzed for 16 PAHs. The average concentrations of Σ_{16}PAH in soils in the surveyed areas were 1142 ng g^{-1} dw, 265 ng g^{-1} dw, 79.7 ng g^{-1} dw, 54.3 ng g^{-1} dw, 54.2 ng g^{-1} dw, 52.3 ng g^{-1} dw, and 36.6 ng g^{-1} dw in Kingtom, Waterloo, Magburaka, Bonganema, Kabala, Sinikoro, and Makeni, respectively. Based on the European soil quality guidelines, Kingtom and Waterloo soils were categorized as heavily and weakly contaminated soil PAHs respectively. The main PAH compounds of this study were 2-ring, 4-ring, and 5-ring PAHs. High molecular weight PAHs (4–6 rings) made up 62.5% of the total PAHs, while low molecular weight PAHs (2–3 rings) was 37.5%. In general, HMWPAHs were predominant in Kingtom, followed by Waterloo. The appointment of PAH sources using different methods revealed mixed sources, but predominantly pyrogenic sources (petroleum, biomass, coal, and fossil fuel contributions). Soil pH has a significant impact on PAH distribution. The toxicity equivalent quantity (TEQ_{BaP}) levels in soils pose a potential health risk to residents in developed cities but pose a negligible health risk to residents in remote cities. This study is significant as its findings reveal the status of PAH soil contamination in Sierra Leone. The results have important implications for policymakers and stakeholders to identify high-risk zones and establish proper environmental monitoring programs, pollution control measures, and remediation strategies to prevent future risks.

Received 13th December 2022
Accepted 27th January 2023

DOI: 10.1039/d2ra07955k

rsc.li/rsc-advances

1. Introduction

Globally, the increasing human population and economic growth, combined with advanced technologies, industrialization, and domestic and agricultural activities, have resulted in the massive generation of waste.[1–3] Polycyclic aromatic hydrocarbons (PAHs) are mutagenic, teratogenic, and carcinogenic organic compounds that have multiple benzene ring structures and are released into the environment by domestic heating, traffic, oil refineries, and industrial processes.[4–6] They are hazardous complex mixtures, bioaccumulative and semi-volatile, and persistently stockpile in the environment (soil, air, sediments, water, *etc.*).[7,8] PAHs can be produced either by natural or anthropogenic sources, including forest fires, volcanic exhalations, diagenesis, industrial emissions, burning of biomass and combustion of fossil fuels, and petroleum spills.[9–11] The Σ_{16}PAH contents have been widely reported in global soil, *e.g.*, in London (400–67 000 ng g^{-1}),[12] Glasgow (48–51 822 ng g^{-1}),[13] Moscow (208–9604 ng g^{-1}),[14] Seville (89.5–4004 ng g^{-1}),[15] Beijing, China (219–27 825 ng g^{-1}),[16] and Delhi, India (81.6–45 017 ng g^{-1}).[17] Soil is a major environmental matrix that sustains the lives of all organisms, whether directly or indirectly, and is a major sink for PAHs due to large areas and retention times, resulting in soil quality degradation worldwide.[18,19] The European soil quality criteria for soil PAH-contamination are grouped into four categories: ΣPAHs < 200 ng g^{-1} indicates no contamination; 200–600 ng g^{-1} indicates partial contamination; 600–1000 ng g^{-1} indicates contamination; and >1000 ng g^{-1} indicates highly contaminated soil.[20] PAH-contaminated soil will gain access to the human system through ingestion or dermic exposure. However, when crops are cultivated on PAH-contaminated soils, they enter the food chain, posing a serious public health risk to humans.[20,21] It has

[a]*State Key Laboratory of Biogeology and Environmental Geology, China University of Geosciences, Wuhan 430074, China. E-mail: shihuaqi@cug.edu.cn; Tel: +86-138-8602-8263*

[b]*School of Environmental Studies, China University of Geosciences, Wuhan 430074, China*

[c]*Chemistry Department, School of Environmental Sciences, Njala University of Sierra Leone, Moyamba District, Sierra Leone 787247*

[d]*School of Management Science and Engineering, China University of Geosciences, Wuhan 430074, China*

† Electronic supplementary information (ESI) available. See DOI: https://doi.org/10.1039/d2ra07955k

been reported that humans exposed to toxic PAHs are most likely to develop asthma, heart disease, and lung cancer.[22–24] Recent research has focused on PAHs due to their potential carcinogenicity and hazardous effects on human health and the ecosystem.[25,26] The US Environmental Protection Agency (USEPA) has listed sixteen PAHs as "priority pollutants", where seven of them have been identified as carcinogens.[27] Scientists have recommended using clean energy as a potential step toward contaminant remediation.[28,29] Nonetheless, environmental scientists and technologists face numerous challenges in the remediation of PAH contaminants in the environment due to the health risks associated with PAH contamination in the environment.[30,31] The fight against the debilitating effects of environmental pollution is very important and should be the concern of every country and stakeholder. Sadly, environmental contaminants and public health issues remain challenging in most developing nations, including Sierra Leone. As a result, it is critical to monitor PAH levels in soil and keep pollutants discharged within recommended limits.[32]

Sierra Leone in West Africa is suffering from numerous environmental problems (soil, water, and air pollution) due to the lack of an adequate environmental quality monitoring system. According to[33] combustion activities, untreated municipal solid waste dumping, automobile emissions, industrial emissions, wood burning, agricultural activities, and other factors all contribute to Sierra Leone's environmental contamination. Untreated wastes, on the other hand, are illegally dumped and burned in Freetown's major dumpsites at Kingtom and Waterloo, posing some serious environmental pollution problems. These activities are potentially harmful to living organisms since they are PAH generators.[34] Previous research has shown that PAH contamination is present in Sierra Leone. These studies focused on air pollution in Freetown's ambient air[35] or PAH concentrations for both indoor and outdoor air in the western urban areas in Freetown.[36] Despite numerous studies on environmental contamination in other nations, Sierra Leone is likely to be one of many countries whose attempts to address this problem amount to nothing. Furthermore, the lack of sufficient information on the status of PAHs in the soil makes it challenging for policymakers to show the precise level of PAH contamination in soil and the potential health risks they pose to humans and the environment, which contributes to the disregard for contaminant control and prevention measures. For effective remediation, it is important to understand the chemistry of pollutants and their sources; this will enable researchers to understand their behavior in different environmental media (*e.g.*, bulk soil, colloids, sediments, water, *etc.*).

Kingtom and Waterloo are situated in the western urban and rural areas of Freetown, surrounded by open dumpsites and local agricultural farmland. Kingtom is the most populated and traffic-congested area in Freetown, with high wind speeds and atmospheric pressure coming straight from the Atlantic Ocean. Waterloo is 30 km from Freetown, which has recently increased in size due to overpopulation in the commercial capital city. Additionally, the hazardous waste deposited at the dumpsites could be a plausible sink and potential source of PAH contamination. According to a previous report,[37] the estimated waste discharged per day at the Kingtom dumpsite was 207 kg per day or 75.555 tons per year. By-products from agriculture and forestry produce the major sources of wood fuel used; 19.345 tons of wood waste is dumped per year (0.053 tons per day), a ton of wood has a heating value of 14 GJ or 0.014 TJ, and the emission of virgin wood produces about 100 μg TEQ/TJ for air and 20 μg TEQ/TJ for residues.[37] Therefore, it is appropriate to investigate the impacts of contamination sources in developed areas. Bonganema is located in the Southern Province of the Njala University local agricultural farmland area. Makeni, Magburaka, Kabala, and Sinikoro are cities in the Northern Province, the province that produces most of the country's agricultural products. Makeni and Magburaka are situated in swampy areas along the Rokel River, while Sinikoro and Kabala are located in the Loma Mansa Mountain basin enclosed by mountains exhibiting condensation properties similar to high latitude areas, so it might develop into a significant PAH reservoir.[11] Furthermore, the swampy and mountainous areas in the Northern Province are partially undeveloped, with natural environments and less densely populated areas, which makes it appropriate to investigate the impacts of contamination sources in remote areas. Yet, information on the status of PAH distribution and the potential health risks posed to humans exposed to PAH-contaminated soil in the studied areas is unknown; thus, it is necessary to investigate the status of PAH in these environments. Therefore, this study investigates the 16 USEPA priority PAHs in the soil to reveal the status and distribution levels of PAH, identify the potential sources of PAH using molecular diagnostic ratios, evaluate the potential risk, and determine the physicochemical properties of soil that influence PAH concentrations in developed and remote cities. To the best of the authors' knowledge, this research is the first attempt to address the status of PAH in developed and remote areas in Sierra Leone. This study is significant as its results reveal the current status of PAH in Sierra Leone. We hope these results will have a significant impact on policymakers and stakeholders in identifying high-risk areas and designing environmental monitoring programs and pollution mitigation and remediation strategies to prevent potential risks and encourage more research in high-risk areas.

2. Materials and methods

2.1. Study area and sample collection

Sierra Leone is a state in West Africa that borders Liberia to the south and Guinea to the north. It is situated on the Atlantic Ocean's west coast with longitudes of 10.21 to 13.32° W and latitudes of 6.91–10.08° N Fig. 1. It has a total area of 71 740 km^2 (27 699 sq. mi). According to the 2015 census report, it has a population of 7 092 113 people.[38] The climate is tropical, hot, and humid throughout the year, with two distinct seasons: dry and rainy. The average temperatures during the dry and rainy seasons range from 25–27 °C and 22–25 °C, respectively. The rainy and dry seasons are from May to October and November to April, respectively. The primary precipitation is tropical rainfall of 5000 m^2 along the coast and 2000 m^2 along the backland.

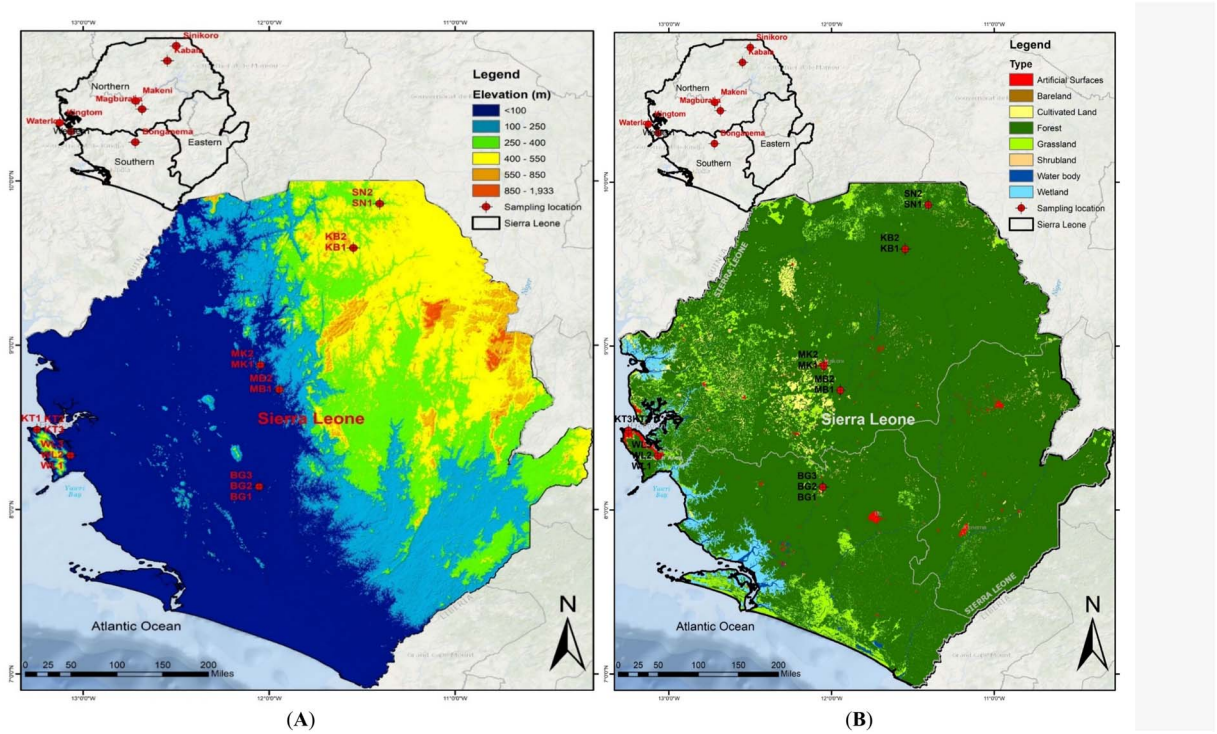

Fig. 1 The map of Sierra Leone illustrates the sampling sites in the topography (A) and the land use type (B). KT: Kingtom; WL: Waterloo; BG: Bonganema; MB: Magburaka; MK: Makeni; KB: Kabala; SN: Sinikoro.

Heavy rainfall characterizes the wet season, whereas hot sunshine and dust-laden trade breezes from the Sahara Desert characterize the dry season. The sample collection was conducted during the wet/rainy season. During the rainy/wet season, runoff from surface soil into groundwater may transport significant loads of PAH contaminants into groundwater, creating a non-point pollution source that jeopardizes groundwater quality.[39] The primary source of drinking water in Sierra Leone, like many other African countries, is groundwater. When it rains heavily, the system's soil becomes a net source of PAHs rather than a net sink. The amount of PAH enrichment in the soil is different for each PAH compound and depends heavily on runoff and soil erosion processes.[40] Text S1 gives a detailed description of the study area, while Table S1† shows the population densities of the study area.

Seventeen topsoil (0–20 cm) samples were collected from six major geographic cities in Sierra Leone (September to October 2019) during the rainy season. The six cities were subdivided into three administrative divisions: Freetown, the commercial capital city including western urban (Kingtom) and rural (Waterloo); southern province (Bonganema); northern province, including Makeni, Magburaka, Kabala, and Sinikoro. A global positioning system (GPS) was used throughout the sampling procedure to correctly record the sampling sites' geographical coordinates in the field. Using a cleaned stainless-steel scoop, at each sampling site, 5 subsamples were collected and fully combined to form a homogeneous composite sample within a 2 m plot: east, west, south, north, and a central point. Prior to being stored in an ice-cold box, each composite sample weighed around 200 grams and was coated immediately in aluminum foil, stored separately, and sealed in labeled polythene bags. The samples were subsequently frozen and transported to the laboratory. Before extraction, the samples were sealed and frozen at −18 °C until pre-treatment within 30 days. Before extraction and chemical analysis, the samples were defrosted, air-dried, and sieved through a <2 mm mesh sieve.

2.2. Chemical analysis, analytical procedures, and sample preparation

The soil samples were tested for the following 16 USEPA priority PAHs: acenaphthene (Ace), benzo (ghi)perylene (BghiP), anthracene (Ant), acenaphthylene (Acy), benzo(*a*)anthracene (BaA), benzo(*b*)fluoranthene (BbF), chrysene (Chr), dibenzo(*a*,*h*) anthracene (DahA), benzo(*k*)fluoranthene (BkF), fluorene (Flo), fluoranthene (Fluo), indeno (1,2,3-*cd*) pyrene (IcdP), benzo(*a*) pyrene (BaP), naphthalene (Nap), pyrene (Pyr) and phenanthrene (Phe). Analytical procedures and sample preparation methods in this research were comparable to those mentioned in previous reports.[5,11,40–42] The samples were quantitatively analyzed by gas chromatography-mass spectrometry (GC-MS, Agilent 6890N GC-5975 MSD) for the 16 PAHs. Text S2 gives a detailed description of the chemical analysis, analytical procedures, and sample preparation.

2.2.1 Soil particle-size distribution and pH analysis. Soil particle distribution and pH were tested in seventeen ($n = 17$) surface soil (0–20 cm) samples in survey areas. The particle-size distribution using a Mastersizer-3000 analyzer (Malvern, England) was determined for sizes ranging from 0.01–3500 μm.

The analysis was similar to that reported previously.[5] Briefly, 10 g of soil sample was dried and subsequently tested with 10% of 10 mL H_2O_2 (Sinopharm, China) and 5% of 10 mL HCl (Sinopharm, China) to eliminate organic substances and carbonates, respectively. After 24 hours of analysis, we separated the residue from the sub-samples and added distilled water. To eliminate the residual acid, this step was repeated by adding 1% of $(NaPO_3)_6$ mixture (Sinopharm, China) to prevent particle aggregation. A potentiometric glass electrode was used to determine the soil pH using a soil/water ratio of 1 : 2.5 (w/w); this method is similar to that reported previously.[43] Briefly, 10 grams of each soil sample and 25 mL of ultrapure water were shaken for 30 minutes and then centrifuged at 4000 rpm for 10 minutes. The pH of the supernatant was measured three times and the average pH value was obtained for each sample. The descriptive statistics of the analytical results of soil particle size and pH were calculated and summarized in Table S5.†

2.3. Quality assurance and quality control

During pre-treatment and instrumental analysis, surrogate standards, and lab and field duplicate procedure blanks were analyzed for quality assurance (QA) and quality control (QC). The surrogate recoveries (mean ± standard deviation) were 46.4 ± 12.0%, 79.7 ± 15.7%, 93.4 ± 15.8%, 96.8 ± 17.5% and 98.1 ± 28.1% for naphthalene-d8, acenaphthene-d10, phenanthrene-d10, chrysene-d12, and perylene-d12, respectively. The relative standard deviation (RSD) between parallels for all target compounds was 21.1 ± 13.2%. No target compounds were detected in the solvent blank samples. All PAH sample concentrations were corrected by surrogate recovery after subtracting the results of procedure blank samples. The analytical quantification limit (QL) in soil varied from 0.11–3.1 ng g^{-1} dw. Method detection limits (MDL) in soil varied from 0.03–0.91 ng g^{-1} dw, which were determined based on 3 times the standard deviations of the procedure blank samples. The quantification limit (QL) was 10 times the procedure blank samples' standard deviations and ranged from 0.11–3.1 ng g^{-1} dw (Table 1).

2.4. The toxicity assessment of PAHs

The relative carcinogenicity of PAH compounds was calculated using the toxicity equivalency factors (TEF).[44] Seven out of the 16 chemicals on the 16 USEPA priority list are considered carcinogens, including BaP, BkF, BbF, Chr, DahA, BaA, and IcdP, which are very toxic and can lead to cancer based on the International Agency for Research on Cancer classification.[45] The different TEF values produce different TEQ values. According to a previous report,[44] the TEF is used to quantify the potencies of PAH compared to BaP and calculate the concentration of the toxicity equivalent quantity (TEQ_{BaP}).[44] Based on the International Agency for Research on Cancer, the TEF values of the 7 PAH carcinogens such as Chr, DahA, BaP, BkF, BbF, BaA, and IcdP are 0.01, 1, 1, 0.1, 0.1, 0.1, and 0.1, respectively. The relative potencies of other PAHs were determined using BaP, which is the most hazardous PAH used to identify carcinogenic factors amongst the potential PAH carcinogens because it has enough toxicological data.[44] The TEF value of 1.0 represents carcinogenic PAHs, while the value of zero represents noncarcinogenic PAHs.[44] The toxicity equivalent quantity (TEQ_{BaP}) concentration for individual samples can be used to calculate BaP toxicity in soil using eqn (1) below.[46] The BaP carcinogen is used as the surrogate compound to approximate the potential cancer risks posed by individual PAH compounds.

$$TEQ_{BaP} = \sum_{i=1}^{7} TEF \times C_{PAHi} \quad (1)$$

where C_{PAHi} is the concentration of the ith exposure to these environments PAH in the soil.

2.5. Statistical analyses and data processing

The statistical analysis of the PAH results was calculated in dry weight to ensure the data were appropriate for the analysis. All target compounds were detected with varying concentrations. A 2-tailed test of significance was used to determine the correlation coefficient at $p < 0.05$. The degree of association between PAH concentrations and soil properties was analyzed using Spearman's correlation coefficients. Additionally, all statistical analyses were achieved *via* Excel 2016 (Microsoft) and SPSS 25.0 (IBM), and ArcGIS 10.5 (Esri) was used in creating the study area and land use maps. All figures were plotted using Origin 2022b (OriginLab).

3. Results and discussion

3.1. PAH occurrence in the soil

The descriptive statistics of the Σ_{16}PAH concentration in the surface soil (0–20 cm) profile are summarized in Table 1. The Σ_{16}PAH concentration levels in soil varied with significant differences across the studied areas from 698–1750; 168–389; 24.9–123; 25.8–81.4; 42.4–64.3; 45.5–59.1; and 24.1–49.0 (ng g^{-1} dw) in Kingtom (KT), Waterloo (WL), Magburaka (MB), Kabala (KB), Bonganema (BG), Sinikoro (SN), and Makeni (MK), respectively. Our investigation revealed that all 16 PAH compounds were detected in KT and WL, though with varying concentrations (see Table 1). However, BbF (in SN) and BbF and BaP (in MK) were not detected. Overall, the content of PAH compounds in this study showed that PAH compounds were ubiquitous in KT, followed by WL, contributing to 71.2% and 16.5% of the total, respectively (Fig. S1†). Based on the European soil quality criteria for PAH contaminants in the environment, KT soil is categorized as heavily PAH-polluted soil, while WL soil is categorized as partially contaminated by PAH, with total PAH concentrations of 1750 ng g^{-1} dw and 389 ng g^{-1} dw, respectively Table 1. The highest total concentrations of 16 PAHs in each site were as follows: MB (123 ng g^{-1} dw), KB (81.4 ng g^{-1} dw), BG (64.3 ng g^{-1} dw), SN (59.1 ng g^{-1} dw), and MK (49.0 ng g^{-1} dw); remote cities, were all categorized as not PAH-contaminated soil.[47] The total PAH concentrations were predominant in the western KT and WL as compared to those in the remote cities. Spearman's correction was used to determine the relationship between the total PAH concentration and population size. A 2-tailed test of significance was used to determine the correlation coefficient, and the correlation

Table 1 The descriptive statistics summary of 16 PAH concentrations (ng g^{-1} dw) in the surface soil (0–20 cm) of the studied areas[a]

PAHs	PAHs-ring	QL	MDL[b]	TEF[c]	Kingtom		Waterloo		Bonganema		Magburaka		Kabala		Makeni		Sinikoro	
					Mean	Range	Mean	Range	Mean	Range	Mean	Range	Mean	Range	Mean	Range	Mean	Range
Nap	2	3.10	0.91	0.001	189	75.5–269	67.8	35.0–114	24.4	21.1–28.0	36.1	9.73–62.4	30.3	10.5–50.1	19.2	8.75–29.7	29.8	27.5–32.1
Acy	3	0.86	0.26	0.001	12.0	9.04–15.9	2.21	1.11–3.25	0.847	0.639–1.08	1.05	0.759–1.34	0.867	0.612–1.12	0.813	0.741–0.885	0.888	0.706–1.07
Ace	3	2.10	0.63	0.001	7.64	3.51–9.96	3.40	2.02–4.89	1.25	0.914–1.71	1.26	1.07–1.45	1.31	0.866–1.76	1.27	1.27–1.27	0.507	ND – 1.01
Flo	3	2.60	0.78	0.001	13.2	8.70–16.6	4.52	4.16–5.16	2.95	2.58–3.55	2.25	2.10–2.40	3.12	1.62–4.63	2.90	2.33–3.47	2.55	2.46–2.65
Phe	3	2.60	0.77	0.001	100	80.2–115	28.5	17.8–38.0	12.2	9.18–13.9	6.85	5.73–7.98	8.47	5.16–11.8	5.87	5.42–6.31	8.44	7.32–9.55
Ant	3	0.32	0.10	0.01	15.8	12.5–18.9	3.93	3.89–4.00	1.58	1.01–2.70	0.804	0.473–1.14	0.924	0.544–1.31	0.499	0.292–0.706	1.02	0.747–1.30
Fluo	4	1.60	0.49	0.001	96.8	69.0–140	29.0	19.9–44.9	4.60	2.85–5.52	3.65	1.12–6.17	2.27	1.94–2.60	1.78	1.61–1.95	3.04	2.35–3.73
Pyr	4	0.37	0.11	0.001	92.8	62.9–136	27.1	18.1–40.1	3.28	2.17–4.32	3.13	0.925–5.34	1.65	1.30–2.00	1.50	1.40–1.60	2.12	1.58–2.66
BaA	4	0.72	0.22	0.1	58.4	28.1–107	9.78	6.00–16.2	0.423	0.380–0.500	2.03	0.370–3.68	0.493	0.464–0.523	0.545	0.453–0.636	0.539	0.429–0.648
Chr	4	0.11	0.03	0.01	100	59.2–15	26.2	17.8–35.2	0.962	0.658–1.31	4.61	1.05–8.17	1.71	1.40–2.02	1.09	0.894–1.29	1.28	0.851–1.70
BbF	5	0.95	0.29	0.1	85	57.5–140	12.7	7.62–19.0	0.317	ND – 0.340	6.00	ND – 6.00	0.805	0.507–1.10	ND	ND	ND	ND
BkF	5	0.45	0.14	0.1	60.3	40.3–97.9	10.3	7.6–14.1	0.407	0.295–0.527	2.26	0.710–3.81	0.641	0.556–0.726	0.417	0.403–0.431	0.698	0.498–0.897
BaP	5	2.90	0.63	1	106	64.3–187	18.8	11.8–25.7	0.715	ND – 0.715	4.91	ND – 4.91	0.889	ND – 0.889	ND	ND	0.754	0.705–0.802
IcdP	5	0.22	0.07	0.1	86.8	56.9–141	6.10	4.25–8.28	0.143	ND – 0.183	1.90	0.387–3.41	0.272	0.0838–0.461	0.274	ND – 0.274	0.073	0.073–0.074
DahA	6	0.15	0.05	1	15.9	2.72–33.0	1.57	1.06–1.99	0.158	0.149–0.174	0.404	0.250–0.557	0.267	0.225–0.310	0.152	0.059–0.245	0.173	0.116–0.230
BghiP	6	0.27	0.08	0.01	102	67.6–163	13.1	9.69–15.2	0.113	0.092–0.126	2.527	0.273–4.78	0.0860	ND – 0.0860	0.200	ND – 0.200	0.431	0.164–0.699
Σ_{16}PAHs[d]					1142	698–1750	265	168–389	54.3	42.4–64.3	79.7	24.9–123	54.15	25.8–81.4	36.6	24.1–49.0	52.3	45.5–59.1
Σ_7PAHs[e]					513	308–866	85.4	56.5–120	3.12	2.59–3.75	11.9	13.7–30.5	4.18	3.24–6.03	2.48	2.09–2.88	3.51	2.67–4.35
LMW-PAHs[f]					338	189–445	110	64.1–169	43.2	35.4–50.6	48.3	19.9–76.7	45.0	19.4–70.7	30.6	18.8–42.4	43.2	38.8–47.7
HMW-PAHs[g]					805	508–1305	155	104–221	10.5	6.60–13.7	26.0	5.10–46.8	8.60	6.60–10.7	5.77	5.29–6.60	9.10	6.80–11.4

[a] ND: not detected; QL: quantification limit. [b] Method detection limit. [c] Toxicity equivalent factor. [d] Total concentrations of 16 individual PAH. [e] Total concentration of carcinogenic compounds. [f] Low-molecular-weight PAHs. [g] High-molecular-weight PAHs.

coefficient value was used at $p < 0.05$. The total Σ_{16}PAHs concentration had a strong positive correlation with the total population ($r = 0.976$, at $p < 0.05$) (Table S1a and Fig. S2†). This suggests that human activities associated with biomass combustion of waste incineration, domestic heating and local farming contributed to the high PAH contents in KT, followed by WL, and more care should be taken to prevent their residents and their environments from becoming polluted. Fig. 2 illustrates the mean concentration distribution levels of the carcinogenic (Σ_7PAH) compounds in the soil and their detection frequencies in the following order: BaP (34.77), >BbF (27.49), >Chr (23.48), >IcdP (18.91), >BkF (13.01), >BaA (12.53), and DahA (3.22). The results show that among the carcinogens, BaP, which is the most potent PAH, displayed the highest mean concentration level. Although the mean concentration of DahA was the lowest, it was detected with a detection frequency of 100%, and BaP had a detection frequency of 64.7% (Fig. 2).

The PAH levels investigated in this study were compared to those reported in other parts of the world in Table S2.† The total PAH mean concentration observed in KT soil (1142 ng g^{-1} dw) was significantly higher than those found in urban soils in Turin (857 ng g^{-1} dw), Italy;[13] rural areas (333 ng g^{-1} dw), southern Italy;[48] Dajiuhu (42.4 ng g^{-1} dw), central China;[11] and Caserta provincial territory (84.9 ng g^{-1} dw), southern Italy.[32] Nonetheless, PAH levels in our research were lower as compared to other world regions, including Shenyang (2370 ng g^{-1} dw), China;[49] Beijing urban areas (3917 ng g^{-1} dw), China;[16] Glasgow urban areas (11 930 ng g^{-1} dw), UK;[13] Delhi rural areas (1910 ng

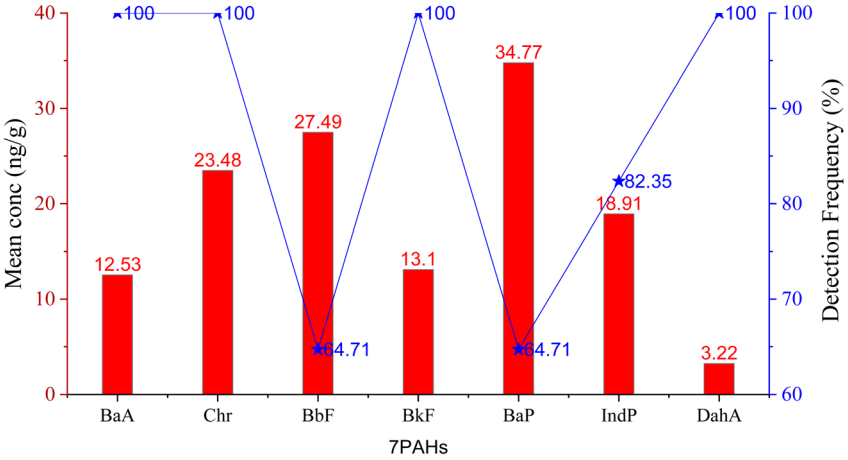

Fig. 2 Mean concentration distribution of the carcinogenic (Σ_7PAH) compounds and detection frequency in the soil profile.

g^{-1} dw), India;[50] Delhi urban areas (6838.6 ng g^{-1} dw), India;[17] London urban areas (18 000 ng g^{-1} dw), UK[12] and Moscow urban areas (1553.9 ng g^{-1} dw), Russia[14] (Table S2†). In general, these studies collectively reported the proximity of anthropogenic activities such as combustion, industrialization, agriculture, economic growth, land use, and densely populated urban areas to enhance PAH pollution. Furthermore, the total PAH mean concentration in WL (265 ng g^{-1} dw) was significantly greater than those found in Hong Kong rural areas (57.6, ng g^{-1} dw), China.[51] Additionally, the PAH concentrations in MK, MB, KB, and SN were all lower than those found in Kumasi, Ghana,[52] Dajiuhu, China,[11] and the Caserta province in southern Italy.[32]

3.2. Spatial distribution and PAH-ring composition

The spatial distribution of PAH concentration in the topsoil profile displayed a significant difference across the studied areas. The total average levels of the Σ_{16}PAH in the soil of the surveyed areas varied significantly as follows: 1142.4 ng g^{-1} dw, 265.1 ng g^{-1} dw, 79.7 ng g^{-1} dw, 54.3 ng g^{-1} dw, 54.1 ng g^{-1} dw, 52.8 ng g^{-1} dw, and 36.5 ng g^{-1} dw in KT, WL, MB, BG, KB, SN, and MK, respectively. The highest PAH mean levels were found in KT, followed by WL. Fig. S3† and 3 show the fractional contributions of the PAH compounds extracted. Nap was the main PAH compound in all the samples, which corroborates the results presented in Fig. S1† and Table 1. The PAH compounds with the highest total mean concentrations were Nap (189 ng g^{-1}) and BaP (106 ng g^{-1}) in KT (Table 1). In general, the distribution and concentration level of Nap was highly detected across the surveyed areas, though with different concentration levels (Fig. 3). The individual PAH percentage composition distribution in this study revealed that KT contributed more to the concentrations of four-, five-, and six-ring PAH compounds as compared to WL, while sites MK, SN, BG, and MB contributed more to two- and three-ring PAH compounds (Fig. 3). The concentrations of 4–6-ring PAHs were abundant at KT, followed by WL dumpsites can be associated with pyrogenic PAH pollutants from combustion and possibly the soil physico-chemical property distribution. The findings in our study are in agreement with those reported previously.[53] It was observed that anthropogenic activities contributed to more PAH pollutants at KT, followed by WL. These activities could be potentially harmful to living organisms and the ecosystem to a certain extent since they are PAH generators.[34] Conversely, in remote cities, petroleum pollution caused the formation of PAHs. This observation is in agreement with a previous report.[5]

The distribution patterns of different PAH-ring compounds and their percentage compositions varied significantly across the surveyed areas as follows: 4-ring > 5-ring > 2-ring > 3-ring > 6-ring-PAHs with mean values of 83.03 ng g^{-1}, 69.97 ng g^{-1}, 63.21 ng g^{-1}, 43.19 ng g^{-1}, and 23.92 ng g^{-1}, contributing to 29.30%, 24.70%, 22.31%, 15.24%, and 8.44% of the total, respectively (Fig. 4). The total PAH-ring composition indicated that 2-ring, 4-ring, and 5-ring- PAHs were the main PAH compounds in this study. The concentration of 4-ring PAH (348.17 ng g^{-1}) was the highest in KT, followed by 5-ring (338.43 ng g^{-1}), 2-ring (188.98 ng g^{-1}), 3-ring (148.91 ng g^{-1}), and 6-ring (117.88 ng g^{-1}), which contributed 30.48%, 29.62%, 16.54%, 13.04%, and 10.32% of the total, respectively (Fig. 4 and Table S3†). This observation suggests that the high input of combustion at the KL followed by WL in sites might be a potential source of pollution for PAH in the dry season. The concentration of 4-ring PAH (92.11 ng g^{-1}) was abundant in WL, followed by 2-ring (67.83 ng g^{-1}), 5-ring (47.91 ng g^{-1}), 3-ring (42.60 ng g^{-1}), and 6-ring (14.67 ng g^{-1}), contributing to 34.74%, 25.59%, 18.07%, 16.07%, and 5.53% of the total, respectively. The concentration of the 2–3-ring PAH was predominant in BG, MK, KB, and SN agricultural soils. The concentrations of 2-ring PAH were (24.41 ng g^{-1}), (19.25 ng g^{-1}), (30.33 ng g^{-1}), and (29.83 ng g^{-1}), contributing to 45.49%, 53%, 56.56%, and 57% of the total, in BG, MK, KB, and SN, respectively. The concentrations of 3-ring PAH were (18.78 ng g^{-1}), (11.34 ng g^{-1}), (14.70 ng g^{-1}), and (13.41 ng g^{-1}), contributing to 34.99%, 31.24%, 27.42%, and 11.41%, of the total, in BG, MK, KB, and SN, respectively. The concentration of 2-ring PAH (36.07 ng g^{-1}) was prevalent in MB, followed by 4-ring (13.42 ng g^{-1}), contributing to 48.58%, and 18.07%, of the total, respectively in Fig. 4 and Table S3.† This supports the fractional distribution shown in Fig. 3.

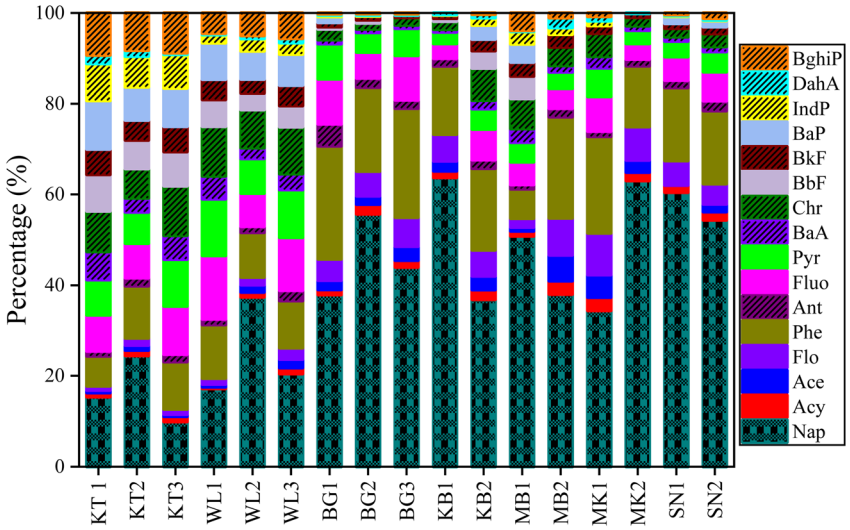

Fig. 3 The individual PAH concentrations and percentage composition in the topsoil from selected cities in Sierra Leone. KT: Kingtom, WL: Waterloo: BG: Bonganema, MB: Magburaka, MK: Makeni, KB: Kabala, and SN: Sinikoro.

In Fig. 4, 2–3-ring PAH compounds were abundant in BG, MK, SN, and KB, which might be produced by petroleum combustion processes. However, in contrast to KT and WL, remote cities in these areas had fewer human activities. This suggests that high temperatures may lead PAHs to move from particulate matter and enter the vapor phase, and they are easily transported to the atmosphere in remote areas.[54] This observation is in agreement with findings reported for agricultural soils[54] in India. Due to the relative abundance of LMW-PAH and high solubility, 2–3-ring PAHs are susceptible to being absorbed by the particulate matter in the soil and migrating deep down into the soil by leaching, which could pose a potential risk in the near future.[47,55] In summary, the persistent distribution pattern of PAH-rings was strongly affected by the ring numbers; 4–6-ring PAHs are resistant to degradation due to the abundance of HMW-PAHs over LMW-PAHs in KT, followed by WL. It was hypothesized that apart from degradation, there was only adsorption in the migration process of PAHs, and the concentration of PAHs in the solid phase had achieved adsorption equilibrium with the liquid phase.[56] Therefore, the abundance of 2–3-ring PAHs in soils in remote cities can easily adsorb PAHs in soils to create a smooth migration process with increasing soil depth as compared to sites in developed cities.

The distribution patterns of LMW and HMW-PAHs concentration levels in the soil across the surveyed areas were also evaluated. The total mean concentration of LMW-PAHs was 338, 110, 43.2, 48.3, 45.0, 30.6, and 43.2 ng g^{-1} dw in KT, WL, BG, MB, KB, MK, and SN, respectively. While HMW-PAHs were 805, 155, 10.5, 26.0, 8.60, 5.77, and 9.10, ng g^{-1} dw in KT, WL, BG, MB, KB, MK, and SN, respectively, as shown in Table 1.

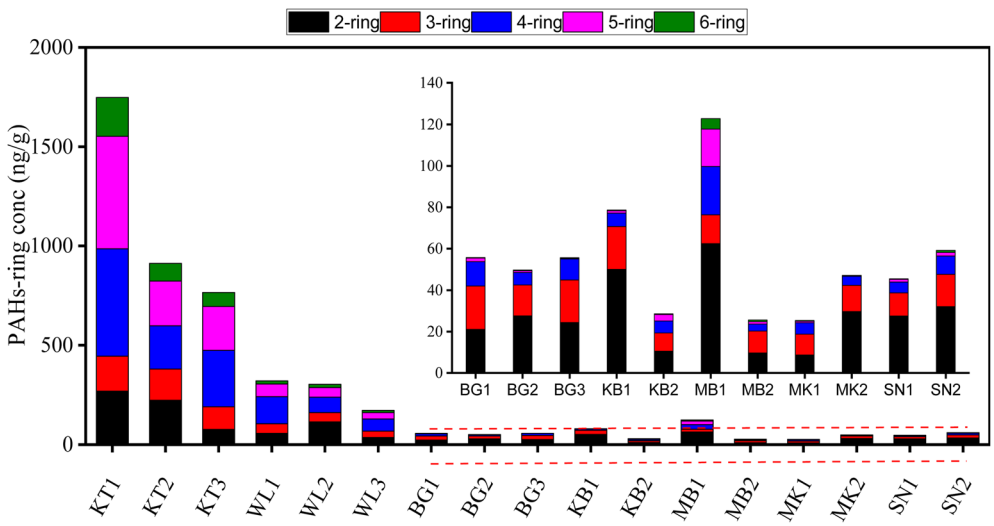

Fig. 4 The concentrations of 2–6-ring PAHs in the topsoil sample. KT: Kingtom, WL: Waterloo: BG: Bonganema, MB: Magburaka, MK: Makeni, KB: Kabala, and SN: Sinikoro.

Generally, larger amounts of HMW-PAHs were observed in developed cities as compared to remote cities. Overall, the content of HMW-PAHs was markedly high in KT compared to WL than other cities. A further regrouping of PAHs showed that HMW-PAHs (4–6 rings) contributed 62.5%, whereas LMW-PAHs (2–3 rings) contributed 37.5% of the total extracted PAHs (Fig. S4†). Nevertheless, the DF of LMW-PAHs (99.02%) was higher than HMW-PAHs (90.59%). Results in Table S3† show that KT and WL made up 29.58% and 41.66% of LMW-PAHs composition, respectively. In comparison, HMW-PAHs contributed 70.42% and 58.3% of the total extracted PAHs in KT and WL, respectively. WL recorded a high LMW-PAHs percentage composition as compared to KT, but the reverse was observed for the HMW-PAHs percentage composition. However, LMW-PAH compounds were predominant in MK (84.24%), KB (83.98%), SN (82.61%), BG, (80.48%), and MB (65.04%) as compared to HMW-PAHs (15.73%, 16.02%, 17.38%, 19.51%, and 34.97%, respectively). The highest concentration of LMW-PAH was found in MK, followed by KB, and the lowest in MB (Table S3†). Evidence suggests that PAHs are formed naturally in soils with concentrations in the range of 1–10 ng g^{-1}.[57] Our research findings showed that both natural and anthropogenic activities influenced the composition and distribution patterns of PAHs in the surveyed areas. As mentioned above, human activity was the main contributor to the composition of PAHs in the soil in KT, followed by WL, while PAHs in MB, MK, KB, SN, and BG soils were more attributed to natural processes in the environment. PAHs' molecular weight, soil organic matter, and vapor pressure could also influence their mobility in soil.[58,59] For instance, lighter PAHs (2–3 rings) in MB, MK, KB, SN, and BG tend to be more volatile in soil, while heavier ones (4–6 rings) are more favorable for binding with colloidal particles and remain immobilized near the source area.[9,30,60] In summary, the high content of the LMW-PAH in the topsoil (0–20 cm) in MK, KB, SN BG, and MB may have a stronger tendency to move down into the soil as compared to HMW-PAH due to the weak relative affinity for soil organic matter and high-water solubility of LMW-PAH. Additionally, the differential behavior of LMW-PAH in topsoil, including photodegradation and volatilization may contribute to low PAH concentrations in topsoil. There have also been reports that LMW-PAH decreases with increasing soil depth. The high content of HMW-PAH in the topsoil (0–20 cm) in KT, followed by WL suggests a probable input of atmospheric pollution since HMW-PAHs usually originate from combustion.

3.3. PAHs source identification

3.3.1. Compositional pattern method. In our study, the compositional pattern was used to identify the potential source of PAH pollutants in the surface soil. PAHs released from various sources displayed different molecular compositions. The common anthropogenic sources of PAH emission in the environment are combustion and petroleum, which have a significant impact on the PAH emission profiles. Generally, LMW-PAHs are mostly related to petroleum sources, whereas HMW-PAHs are related to combustion. According to a previous report,[61] petrogenic PAHs are normally found in LMW-PAHs, while pyrogenic PAHs are found in HMW-PAHs. It was proposed that a ratio of LMW-PAHs/HMW-PAHs less than 1 implies pyrogenic and greater than 1, suggesting petrogenic sources. In this study, the ratios of LMW-PAH/HMW-PAH values varied from 0.33–8.93, Fig. 5.[62] Almost all the samples from KT and WL had a ratio less than 1, except for the site with code WL2, where the ratio was slightly above 1, indicating that pyrogenic sources of PAHs emission were the main PAH contaminant in KT and WL soils, while samples from BG, MB, KB, SN, and MK showed ratios greater than 1, suggesting petrogenic sources as the primary source of PAH emission in these cities.[62] The data presented in Fig. 3 is in agreement with the spatial distribution results in Fig. S3.† Specifically, the PAHs extracted from sites in KT and WL contained predominantly (>50%) HMW compounds, which suggests a pyrogenic source as opposed to >65% LMW components in samples from other sites, indicating a petrogenic source (Fig. 5).

3.3.2. Molecular diagnostic ratios method. Several source resolution methods are used to identify PAH sources, and one of the most frequently used is the molecular diagnostic ratio method. The main sources of PAHs in the environment include the incomplete combustion of coal, biomass, and other fossil fuels, as well as petrogenic sources. Both natural and anthropogenic processes can result in incomplete combustion, though anthropogenic activities are increasingly becoming the main contributors.[42]

Researchers typically use ratios such as Flu/(Flu + Pyr), BaA/(BaA + Chr), Ant/(Ant + Phe), and IcdP/(IcdP + BghiP) to identify potential PAH pollution sources in soil samples. The ratio of Ant/(Ant + Phe), for values greater than 0.10, indicates pyrogenic/combustion, and less than 0.1, indicates petrogenic/petroleum.[62,63] The ratio of BaA/(BaA + Chr), values from 0.2–0.35 indicates petroleum combustion sources, less than 0.2 indicates petroleum sources, and greater than 0.35 indicates combustion sources.[62,63] The ratio of IcdP/(IcdP + BghiP), for values between 0.2–0.4 suggests petroleum combustion sources, less than 0.2 indicates petroleum sources, and greater than 0.4 implies combustion sources.[62,63] The ratio of Fluo/(Fluo + Pyr) values between 0.40–0.50 indicates petroleum combustion, lower than 0.40 indicates fossil fuel, and above 0.50 indicates coal and biomass combustion.[62,63] In this study, the estimated results for molecular diagnostic ratios for PAH source identification are presented in Fig. 6. In Fig. 6A, the IcdP/(IcdP + BghiP) ratio varied from 0.1–0.84, suggesting mixed sources of PAH emission. KT and WL contributed approximately 57% of the petroleum combustion of total PAHs in the investigated sites and contributed moderately to PAH pollution in MB and SN. BG and MK had ratios above 0.5, suggesting that about 35.7% of PAH pollution was a result of biomass or coal combustion.[62,63] In Fig. 6A, the ratio of Fluo/(Fluo + Pyr) varied from 0.49–0.62, indicating mixed sources with the maximum contribution from petroleum combustion, biomass and coal combustion, and the minimum from petrogenic and fossil fuel combustion.[62,63] In Fig. 6B, the BaA/(BaA + Chr) ratio varied from 0.21–0.4. Approximately 88% of all sampling sites exhibited a ratio from 0.2–0.35, and 11.8% had a ratio greater than 0.35, suggesting

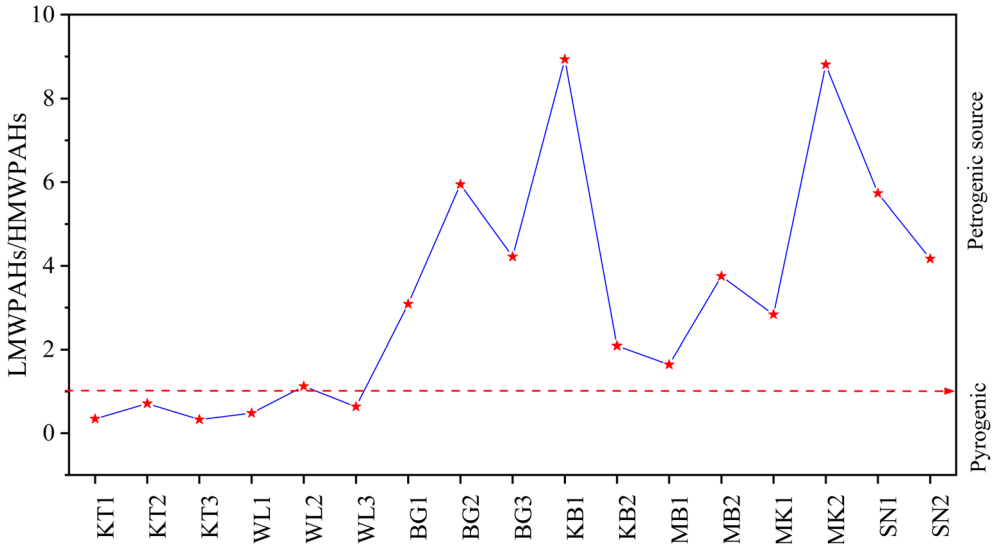

Fig. 5 LWPAH/HWPAH ratios line + symbol diagram of the sampling locations. KT: Kingtom, WL; Waterloo: BG: Bonganema, MB: Magburaka, MK: Makeni, KB-Kabala, and SN, Sinikoro.

mixed sources of PAH pollution emission with maximum contribution from petroleum combustion.[62,63] In Fig. 6C, the ratio Ant/(Ant + Phe) varied from 0.05–0.18. About 47.1% of all sampling sites had ratios >0.1, 29.4% had ratios <0.1, and 23.5% had ratios equal to 0.1. As evidenced by our findings, emissions from pyrogenic sources accounted for the majority of PAH-contaminated soil in the surveyed areas.[62,63]

In summary, the results from the above methods (LMW/HMW, MDR) revealed mixed sources of PAH emission. The LMW/HMW method indicated that pyrogenic sources were predominant in KT, followed by WL due to the high relative composition of HMW-PAH compounds contrary to MK, KB, SN, BG, and MB cities with a high relative abundance of LMW-PAH compounds, indicating petrogenic sources of PAH contamination. MDR results showed coal and biomass, petroleum, and fossil fuel combustion in KT and WL, while petroleum and fossil fuel combustion in KB, MK, and SN, and coal and biomass, and petroleum combustion in MB and BG were the significant contributors to the enrichment of PAHs. Our investigated results for source identification agree with those reported previously.[11]

3.3.3. Principal component analysis. Principal component analysis was employed to identify the different PAH origins and their contributions (Fig. 7). Unlike molecular diagnostic ratio analysis that attributes PAH to combustion sources, PCA can examine specific sources such as traffic emissions, fossil fuel combustion, and coal combustion.[64] Here, components with similar characteristics, such as loading values, were grouped into principal components (*e.g.*, PC1, PC2) depending on their variance percentages and eigenvalues.[65] For the cumulative variance contribution, about 95.5% of the principal components were extracted. As shown in Fig. 7, PC1 contributed to 83.46% of the total PAH variance extracted. It had a strong loading on Nap, followed by Phe, Fluo, Pyr, and Chr, with moderate contributions from BaP, BghiP, Flo, BbF, BkF, IcdP, BaA, Ace, Ant, Acy, and DahA. Nap emissions may be due to the combustion of fossil fuels, the fraction of petroleum products, wood, and crude oil,[66,67] while emissions of Chr, Pyr, and Fluo

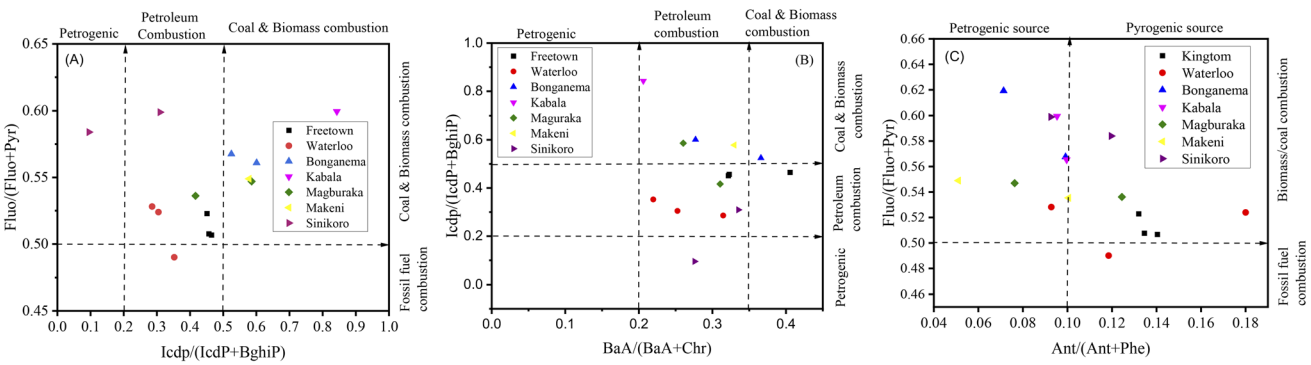

Fig. 6 (A) PAH cross-correlations for the ratios IcdP/(IcdP + BghiP) *versus* Fluo/(Fluo + Pyr), (B) BaA/(BaA + Chr) *versus* IcdP/(IcdP + BghiP), and (C) Ant/(Ant + Phe) *versus* Fluo/(Fluo + Pyr).

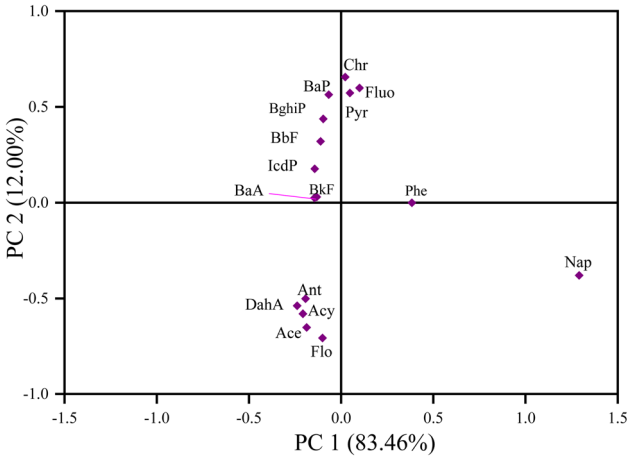

Fig. 7 Loading diagram of principal component analysis in the sample sites' localities.

are commonly associated with diesel exhaust.[68,69] Previous studies indicated that BaP emission is associated with the partial combustion of fossil fuel,[70] IcdP, BghiP, and DahA as indicators of motor vehicle exhaust,[71,72] BkF and BbF are linked to the combustion of fossil fuel,[73] and according to the literature,[74,75] Flo is a crude oil contributor. This result shows that PC1 is a petrogenic source, given that most PAHs emerged from biomass/coal combustion and petroleum and vehicle emissions. Similarly, PC2 accounted for 12% of the aggregate variance. It was loaded on Chr, Fluo, Pyr, BaP, BghiP, BbF, IcdP, BkF, and BaA, while Phe, Nap, Ant, DahA, Acy, Ace, and Flo exhibited fewer contributions. According to a previous report,[76] Chr, Fluo, and Pyr are identified as coal combustion markers, while BbF, BkF, BaA, and BaP are diesel and gasoline emission indicators. Therefore, we recognize PC2 as diesel and gasoline emissions. Overall, the findings of diagnostic ratios and PCA revealed that multiple sources contributed to PAH pollution in this research. However, the predominant sources were pyrogenic sources such as petroleum, coal, biomass combustion, and traffic emissions.

3.4. Soil texture and pH influencing PAHs distribution

Different pH values may have an impact on soil texture migration or the absorption of PAHs in the soil. In this study, the pH value of the soil had a significant influence on the enrichment of PAH (Fig. 8). The pH values varied between strongly acidic and alkaline soils but the majority of the samples were acidic, except for KT, which was attributed to alkaline pH ranging from 7.8–8.0 with a Gmean of 7.9 (Table S5 and Fig. S6†). Nevertheless, agricultural productivity in an acidic soil environment is more suitable for plant growth than in alkaline soils because they depend more on mineral fertilizers that mostly lead to soil degradation or minimize the availability of nutrients.[77] Our findings revealed that soil pH played a significant role in the enrichment of PAH in soil. The pH correlated significantly with the contents of PAH, with strong significant positive correlations on the 5-ring ($r = 0.77$, $p < 0.05$), 6-ring ($r = 0.74$, $p < 0.05$), and Σ_7PAHs ($r = 0.76$, $p < 0.05$) compared to concentrations of the 2-ring ($r = 0.62$, $p < 0.05$) and LMWPAHs ($r = 0.60$, $p < 0.05$), suggesting that HMW increases with increasing pH values. Predicting the PAH concentration on a single soil-geochemical factor is difficult, so further study is necessary to elucidate the functions of soil texture and pH in PAH sorption.[78] Some global investigations on PAHs soil texture-sized distribution revealed that the soil particle size has different probable factors that might influence the PAHs distribution in the soil, including the environmental conditions of sampling sites, soil chemical properties, the different particle characteristics (*e.g.*, aging and partitioning processes).[79] In this study, soil textures varied between clay-silt and silt-sand in the different studied sites. Soil-texture distribution patterns were silt > clay > sand in KB, MB, MK, SN, and BG; sand > silt > clay in WL and KT. Generally, sand and silt were the dominant soil textures compared to clay across the studied areas. Sand textures were distributed in the following order: WL > KT > MK > SN > MB > BG > KB, which contributed 75%, 59%, 50%, 43%, 36%, 28% and 23%, of the total, respectively (Fig. S5†). It was proposed that relatively high PAH contents were attracted to large particle sizes, while silt and clay were attracted to relatively low PAH concentrations.[79] This hypothesis explains the abundance of sand-sized textures in KT and WL as compared to those in MB, MK, SN, BG, and KB with lower PAH content in the soil. With the contracting PAH distribution pattern between KT and WL, this differential behavior might be associated with different soil-particle structures, the environmental conditions of sampling sites, the input of soil organic matter, and contamination history. Additionally, sand particles normally display poor PAH binding affinity as compared to clay/silt due to decreasing coarse surface area.[79] Besides, we observed that the sand texture was the only texture that correlated significantly with strong positive correlations on 5-ring, 6-ring, and Σ_7PAHs ($r = 0.55$, 0.67, and 0.67, $p < 0.05$), respectively, as compared to 2-ring ($r = -0.24$, $p < 0.01$) and LMWPAHs ($r = -0.29$, $p < 0.01$) (Fig. 8). Silt-texture compositions were distributed as follows: KB > MB > BG > SN > MK > KT and WL, and contributed 46%, 42%, 41%, 39%, 28%, 26%, and 16% of the total, respectively. The silt texture was abundant in KB soils (Fig. S5†). The silt textures correlated significantly with a strong negative correlation on the 5-ring, 6-ring, HMWPAHs, and Σ_7PAHs ($r = -0.59$, -0.70, -0.55, and -0.69 $p < 0.05$), respectively, compared to 2-ring, 3-ring, and LMWPAHs ($r = -0.32$, -0.46, and -0.39, $p < 0.01$), respectively, signifying that the more volatile PAHs were moving towards adsorption equilibrium with soil texture. Clay-textures were distributed as follows: KB > BG > MK > MB > SN > KT and WL, contributing 32%, 31%, 23%, 22%, 19%, 15%, and 9%, of the total, respectively (Fig. S5†). The clay texture was abundant in KB, followed by BG. The clay content correlated significantly with a strong negative correlation on 5-, 6-ring, and Σ_7PAHs ($r = -0.55$, -0.65, -0.65, $p < 0.05$), respectively, compared to 2-ring and LMWPAHs ($r = -0.29$, -0.32, $p < 0.01$), respectively. Overall, the clay-silt textures made significant contributions in KB and BG soils, thus suggesting that PAH in KB and BG soils might have quicker release rates and high bioavailability and size based on their hydrophobicity as compared to WL and KT soils with

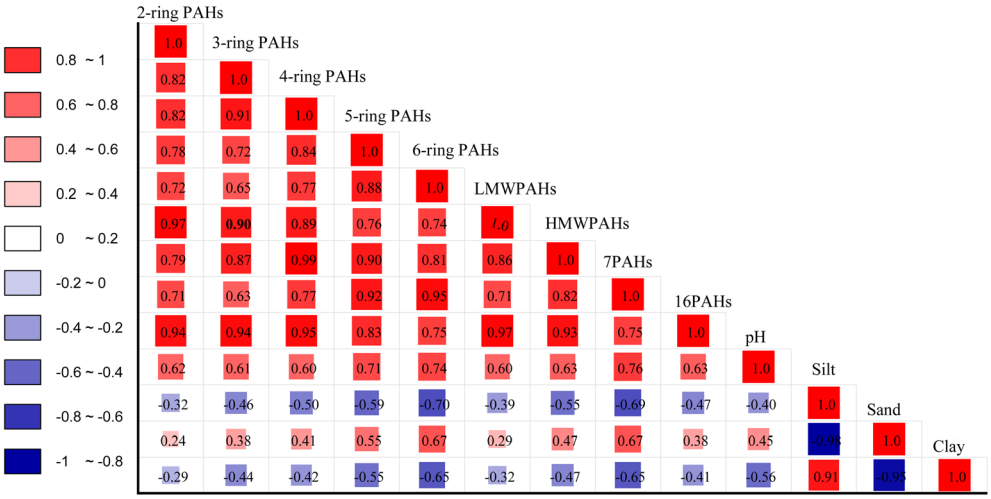

Fig. 8 Spearman's correlation coefficients between PAH concentrations and the physicochemical properties of soil in the studied areas. (Spearman's coefficients at significance levels of $p < 0.05$* and $p < 0.01$**).

a high proportion of sand.[32,77] Moreover, clay-silt particles in KB and BG may have strong PAH binding capacities as compared to MK and SN, and a much stronger binding capacity of PAH than those in WL and KT due to increasing clay-silt particle surface areas. As mentioned above, soil pH was strongly correlated with PAH contents, compared to some studies that investigated high soil organic matter (SOM) with binding capacity at lower pH.[32] Based on their hypothesis, we may assume that high SOM may have binding capacity at lower pH. Hypothetically, the SOM may be protonated at lower pH, thus increasing the hydrophobicity of organic matter in the soil.[32] Moreover, acidic soils may prevent the metabolic activities of microbes, which may significantly contribute to PAH biodegradation;[32] further research on the influence of SOM on PAH distribution in soils of the studied areas will be conducted in the future.

3.5. Toxicity evaluation of PAHs in the soil

In Table 2 and Fig. 9, the toxicity equivalent quotient (TEQ_{BAP}) was evaluated using eqn (1) to determine the hazards of individual and total PAHs. The total TEQ_{BAP} potency in soil varied significantly across the studied areas: 87–273.4 ng g^{-1} dw, 16.5–34.3 ng g^{-1} dw, 1.03–1.14 ng g^{-1} dw, 0.44 ng g^{-1} dw −7.39 ng g^{-1} dw, 0.43–1.59 ng g^{-1} dw, 0.98–1.28 ng g^{-1} dw, and 0.21–0.45 ng g^{-1} dw, with mean values of 153.635 ng g^{-1} dw, 24.90 ng g^{-1} dw, 1.078 ng g^{-1} dw, 6.668 ng g^{-1} dw, 1.452 ng g^{-1} dw, 1.132 ng g^{-1} dw, and 0.326 ng g^{-1} dw in KT, WL, BG, MB, KB., SN, and MN, respectively. Our findings revealed that samples from the urban and rural areas of Freetown exhibited higher mean TEQ_{BAP} toxicity levels in soil, especially KT, followed by WL as compared to TEQ_{BAP} levels in MK, MB, KB, and SN BG cities. Similarly, for cities in the Northern Province, the mean toxicity level of TEQ_{BAP} was high in MB followed by KB as compared to those in SN and MK. Additionally, the lowest TEQ_{BAP} toxicity level was found in MK. The average values of TEQ_{BAP} levels for the potent PAH compounds (Σ_7PAHs) distribution pattern are as follows: BaP > DahA > BbF > IcdP > BkF > BaA > Chr. Overall, the potency of BaP, DahA, and BbF predominated amongst the carcinogenic compounds, with a fractional percentage contribution of 76.6%, 7.10%, and 6.05%, respectively. Comparatively, BaP, which is classified as the most potent carcinogen, contributed the highest portion of human carcinogens, with 83.1%, 14.8%, 1.28%, 0.39%, 0.23%, and 0.19% of the total TEQ_{BAP} in Kingtom, Waterloo, Magburaka, Sinikoro, Kabala, and Bonganema, respectively.

On comparing our results with previous literature worldwide, as shown in Table S4,† the total mean TEQ_{BAP} levels reported in KT were remarkably greater than those in Tarragona[80] of Spain, Campania of southern Italy,[48] and Gwangju City of Korea.[81] However, TEQ_{BAP} levels in KT were lower than those in Delhi, India.[82] Similarly, total TEQ_{BAP} levels reported in WL were substantially greater than those revealed in Norway[83] and Poland's agricultural soils.[84] However, the total soil TEQ_{BAP} levels in WL were lower than those reported in Latium in rural Italy[48] and UK rural areas.[83] Hypothetically, the high TEQ_{BAP} toxicity levels in KT, followed by WL could be linked to the abundance of HWM-PAHs in the TEQ computation, indicating the abundance of pyrogenic emission processes that could be associated with biomass combustion as a result of the massive unsegregated and hazardous waste incineration or car emissions due to traffic congestion at the KT dumpsite and surrounding settlements. It may be concluded that TEQ_{BAP} levels were higher in Kingtom and Waterloo than in Magburaka, Kabala, Sinikoro, Bonganema, and Makeni. In addition, compared to other parts of the world, the total soil TEQ_{BAP} values in Magburaka, Kabala, Sinikoro, Bonganema, and Makeni suggest a low risk to human health.

This study evaluated the status of 16 PAHs in the topsoils of local agricultural farmlands and dumpsite areas, their sources, soil textures, and soil pH impact on PAHs distribution, and subsequently evaluated the potential health risk associated with soil in developed and remote cities in Sierra Leone. Our investigation showed that the KT soil is heavily contaminated with PAH, followed by WL with weakly contaminated soil, which is

Table 2 Toxicity equivalent quantity (TEQ_{BaP}) levels (ng g^{-1} dw) in the topsoil (0–20 cm) of the study areas[a]

PAHs		Kingtom		Waterloo		Bonganema		Magburaka		Kabala		Sinikoro		Makeni	
TEQ[c]	TEF[b]	Range	Mean	Range	Mean	Range	Mean	Range	Mean	Range	Mean	Range	Mean	Range	Mean
Nap	0.001	0.075–0.289	0.189	0.035–0.113	0.068	0.021–0.028	0.024	0.010–0.062	0.036	0.011–0.050	0.030	0.028–0.03	0.030	0.009–0.030	0.019
Acy	0.001	0.009–0.016	0.012	0.001–0.003	0.002	0.001–0.001	0.001	0.001–0.001	0.001	0.001–0.001	0.001	0.001–0.001	0.001	0.001–0.001	0.001
Ace	0.001	0.004–0.010	0.008	0.002–0.005	0.003	0.001–0.002	0.001	0.001–0.001	0.001	0.001–0.002	0.001	0.001–0.001	0.001	0.001–0.001	0.001
Flo	0.001	0.009–0.017	0.013	0.004–0.005	0.005	0.003–0.004	0.003	0.002–0.002	0.002	0.002–0.005	0.003	0.002–0.003	0.003	0.002–0.003	0.003
Phe	0.001	0.080–0.115	0.100	0.018–0.038	0.030	0.009–0.014	0.012	0.006–0.008	0.007	0.005–0.012	0.008	0.007–0.010	0.008	0.005–0.006	0.006
Ant	0.01	0.125–0.188	0.158	0.039–0.040	0.040	0.010–0.027	0.016	0.005–0.011	0.008	0.005–0.013	0.009	0.007–0.013	0.010	0.003–0.007	0.005
Fluo	0.001	0.069–0.140	0.097	0.020–0.045	0.030	0.003–0.006	0.005	0.001–0.006	0.004	0.002–0.003	0.002	0.002–0.004	0.003	0.002–0.002	0.002
Pyr	0.001	0.063–0.136	0.093	0.018–0.040	0.030	0.002–0.004	0.003	0.001–0.005	0.003	0.001–0.002	0.002	0.002–0.003	0.002	0.001–0.002	0.001
BaA	0.1	2.807–10.717	5.842	0.600–1.616	0.980	0.038–0.050	0.042	0.040–0.368	0.203	0.046–0.052	0.049	0.043–0.065	0.054	0.045–0.064	0.054
Chr	0.01	0.592–1.571	1.001	0.178–0.352	0.260	0.007–0.013	0.010	0.010–0.082	0.046	0.014–0.020	0.017	0.009–0.017	0.013	0.009–0.013	0.011
BbF	0.1	5.748–14.071	8.538	0.799–1.897	1.270	ND – 0.034	0.032	ND – 0.599	0.599	0.051–0.011	0.080	ND	ND	ND	ND
BkF	0.1	4.030–9.794	6.029	0.762–1.412	1.030	0.029–0.053	0.041	0.070–0.381	0.226	0.056–0.073	0.064	0.050–0.090	0.070	0.040–0.043	0.042
BaP	1	64.256–187.564	105.980	11.826–25.740	18.800	ND – 0.715	0.715	ND – 4.913	4.913	ND – 0.889	0.889	0.705–0.802	0.754	ND	ND
IcdP	0.1	5.687–14.156	8.677	0.425–0.828	0.610	ND – 0.018	0.014	0.039–0.341	0.190	0.008–0.046	0.027	0.007–0.007	0.007	0.027–0.027	0.027
DahA	1	2.716–32.990	15.877	1.063–1.991	1.570	0.149–0.174	0.158	0.250–0.557	0.404	0.225–0.310	0.267	0.116–0.230	0.173	0.059–0.245	0.152
BghiP	0.01	0.676–1.631	1.020	0.087–0.152	0.130	0.001–0.001	0.001	0.003–0.048	0.025	ND – 0.001	0.001	0.002–0.007	0.004	ND – 0.002	0.001
ΣTEQ_{BaP}		86.946–273.387	153.635	15.887–34.277	24.900	0.273–1.144	1.078	0.436–7.388	6.668	0.427–1.588	1.452	0.982–1.283	1.132	0.178–0.446	0.326

[a] ΣTEQ_{BaP} is the sum of the BaP toxicity equivalent quantity in soil; ND (Not detected). [b] TEF is the toxicity equivalent factor. [c] TEQ is the toxicity equivalent quantity for the individual PAH in the soil.

a serious public health concern. The distribution pattern of PAH concentrations in KT and WL suggests that anthropogenic activities influenced the PAH distribution pattern, compared to MK, KB, SN, MB, and BG. The accumulation of PAHs in sediments and soils is a major cause of groundwater pollution, and the vulnerability of groundwater to contamination poses major public health issues since the contaminants can gain access to the food chain.[85–88] Thus, the high content of PAHs in KT and WL soils reveals that these residents are at a higher risk of contamination as compared to other areas, which demands immediate public health attention and proper sensitization of waste disposal and management practices. The mobility of PAHs, like other contaminants, is highly dependent on their physicochemical properties and environmental factors such as temperature and humidity. Whether they are in the particle-bound or gas phase depends on the molecular weight of the PAHs. For example, LMW PAHs (2–3 rings) are highly volatile and exist more in the gaseous phase,[58,59] indicating that KT and WL dumpsites had fewer PAHs in the gaseous phase due to the abundance of high HMW-PAH compounds (Fig. S3,† Table 1). Conversely, sites BG, MG, KB, MK, and SN soil were predominantly (65–84%) polluted by the volatile LMW PAHs. Soil analysis and the determination of particle-bound PAHs, especially in developing countries, is very important because particulate-bound PAHs have been identified as highly carcinogenic with enhanced mutagenic abilities.[89] The PAH concentration in this study was significantly correlated with soil pH.

Anthropogenic activities contributed to the high total mean TEQ_{BAP} levels observed at these dumpsites, notably at the Kingtom dumpsite. The TEQ_{BAP} concentration based on ecological risk assessment results indicated that KT residents, followed by WL residents, are exposed to potent PAHs through inhaling contaminated smoke or dust, which might be linked to the combustion of biomass through waste burning and domestic wood/coal heating proximity to mechanical garages for motorcycles and vehicles, urbanization, and local agricultural practices. All these activities have negative health implications, especially for children and pregnant women who are more vulnerable to diseases due to compromised immune systems. Residents in the western urban and rural areas of

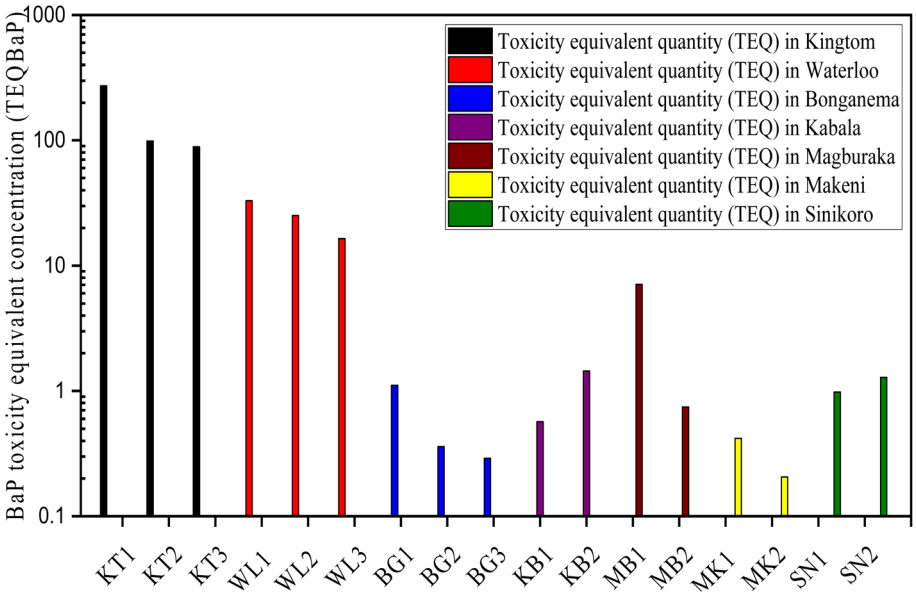

Fig. 9 Variation of the BaP toxicity equivalent quantity (TEQ_{BaP}) values in the sample sites' localities. (Logarithmic scale is applied on the *Y*-axis).

Freetown will continue to face severe health implications if precautionary steps are not implemented, which could pose a serious public health risk. However, PAH contaminants do not solely depend on soil PAH content but also on climate change, soil properties, atmospheric surface particles, topography, vegetation, and so on. Policymakers should consider all the possible relevant factors for pollution control and prevention measures and monitor the activities at these dumpsites, implement the documented laws on waste discharge standards with strict punishment for defaulters and regularly organize programs on pollution control and preventive measures for sensitization, build at least one wastewater treatment plant, and reduce the importation of used vehicles. To conclude, we suggest frequent sampling with different depths/layers, compared with that of surface soil, especially in areas of high potential risk and their nearby communities, to prevent future risks and reservoirs for PAH contaminants.

4. Conclusions

PAHs were found to be ubiquitous at Kingtom, followed by Waterloo dumpsites. The results showed that Kingtom soil was heavily contaminated with significant contributions from 4–5-ring PAHs and Waterloo soil was weakly contaminated with an abundance of 4–2-ring PAHs. However, 2–3-ring PAHs were predominant in remote cities with negligible soil contamination. The persistence of PAHs in Kingtom, followed by Waterloo was primarily influenced by anthropogenic activities. The HMW-PAH concentration was highly significant in developed areas compared to remote areas. There were multiple pyrogenic and petrogenic PAH emission sources but biomass/coal and petroleum combustion sources were predominant. The soil pH was significantly correlated with PAH concentrations. The TEQ_{BaP} levels pose a potential health risk to Kingtom residents, followed by Waterloo residents, and this requires public health attention; however, there are negligible health risks to locals in remote cities. This study presents novel results for the current status of PAH distribution levels in the soil, sources, the impacts of soil properties on PAH concentration, and potential risks in developed and remote areas in Sierra Leone. The findings have important implications that will help policymakers to identify high-risk areas, subsequently improve environmental regulatory policy, and sensitize the public to its importance; this will help prevent potential soil contamination with PAHs and strengthen the prevention and pollution control measures against future risks. We recommend that soils in developed areas should be further analyzed to ensure that the PAH concentrations reported in this research are not being underestimated due to the continued increase in anthropogenic activities in these areas.

Data availability

All data analyzed during this study are included in this paper and the ESI;† also, the raw data that support the results of this article are available on request from the corresponding author upon request.

Author contributions

Mariama Janneh: data curation, investigation, visualization, software, formal analysis, writing—original draft. Yuan Zhang: GC method validation. Chengkai Qu: investigation. Oscar Nkwazema: writing—review, and editing. Xinli Xing: conceptualization, methodology, investigation. Fatuma Nyihirani: formal analysis, data curation. Shihua Qi: conceptualization, writing—review and editing, methodology, resources, supervision. All authors have read and agreed to the published version of the manuscript.

Conflicts of interest

The authors declare that they have no known competing financial interests or personal relationships that could have appeared to influence the work reported in this paper.

Acknowledgements

This paper was financially supported by the National Natural Science Foundation of China (No. 41472257, 41521001) and the Fundamental Research Funds for the Central Universities, China University of Geosciences, Wuhan (No. CUGCJ1702). The authors gratefully acknowledge the authorities and management of Njala University and Dr Yahaya Kudush Kawa in data collection. Additionally, they wish to thank one another for their individual contributions; and a special thanks to Mariama Janneh for sampling assistance.

References

1 Y. He, X. Hu, J. Jiang, J. Zhang and F. Liu, *RSC Adv.*, 2022, **12**, 10825–10834.
2 A. Shitandayi, F. Orata and F. Lisouza, *J. Environ. Prot.*, 2019, **10**, 772–790.
3 P. Li, *Exposure Health*, 2020, **12**, 337–342.
4 A. J. White, P. T. Bradshaw, A. H. Herring, S. L. Teitelbaum, J. Beyea, S. D. Stellman, S. E. Steck, I. Mordukhovich, S. M. Eng, L. S. Engel, K. Conway, M. Hatch, A. I. Neugut, R. M. Santella and M. D. Gammon, *Environ. Int.*, 2016, **89–90**, 185–192.
5 C. Cheng, T. P. Hu, W. Liu, Y. Mao, M. Shi, A. Xu, Y. Su, X. Li, X. Xing and S. Qi, *Environ. Pollut.*, 2021, **291**, 118173.
6 A. Hanedar, E. Güneş, G. Kaykioğlu, S. Ö. Çelik and E. Cabi, *Environ. Monit. Assess.*, 2018, **191**, 42.
7 H.-W. Yuan, J.-F. Chen, Y. Ye, Z.-H. Lou, A.-M. Jin, X.-G. Chen, Z.-P. Jiang, Y.-S. Lin, C.-T. A. Chen and P. S. Loh, *Journal of Marine Systems*, 2017, **174**, 78–88.
8 R. Zhou, L. Zhu, K. Yang and Y. Chen, *J. Hazard. Mater.*, 2006, **137**, 68–75.
9 Z. Qian, Y. Mao, S. Xiong, B. Peng, W. Liu, H. Liu, Y. Zhang, W. Chen, H. Zhou and S. Qi, *Ecotoxicol. Environ. Saf.*, 2020, **196**, 110542.
10 C. Qu, S. Albanese, J. Li, D. Cicchella, D. Zuzolo, D. Hope, P. Cerino, A. Pizzolante, A. L. Doherty, A. Lima and B. De Vivo, *Sci. Total Environ.*, 2019, **674**, 159–170.
11 X. Xing, Y. Mao, T. Hu, Q. Tian, Z. Chen, T. Liao, Z. Zhang, J. Zhang, Y. Gu, S. ul ain Bhutto and S. Qi, *J. Geochem. Explor.*, 2020, **208**, 106393.
12 C. H. Vane, A. W. Kim, D. J. Beriro, M. R. Cave, K. Knights, V. Moss-Hayes and P. C. Nathanail, *Appl. Geochem.*, 2014, **51**, 303–314.
13 E. Morillo, A. S. Romero, C. Maqueda, L. Madrid, F. Ajmone-Marsan, H. Grcman, C. M. Davidson, A. S. Hursthouse and J. Villaverde, *J. Environ. Monit.*, 2007, **9**, 1001–1008.
14 G. Agapkina, P. Chikov, A. Shelepchikov, E. Brodskiy, D. Feshin, N. Bukhanko and S. Balashova, *Moscow Univ. Soil Sci. Bull.*, 2007, **62**, 149–158.
15 E. Morillo, A. S. Romero, L. Madrid, J. Villaverde and C. Maqueda, *Water, Air, Soil Pollut.*, 2008, **187**, 41–51.
16 L. Tang, X.-Y. Tang, Y.-G. Zhu, M.-H. Zheng and Q.-L. Miao, *Environ. Int.*, 2005, **31**, 822–828.
17 B. Kumar, A. Sharma, A. Tyagi, R. Gaur, V. Verma, S. Singh, S. Kumar and C. Sharma, *Arch. Appl. Sci. Res.*, 2012, **4**(4), 1906–1914.
18 S. Singh and A. K. Haritash, *Int. J. Environ. Sci. Technol.*, 2019, **16**, 6489–6512.
19 A. Ukalska-Jaruga, K. Lewińska, E. Mammadov, A. Karczewska, B. Smreczak and A. Medyńska-Juraszek, *Molecules*, 2020, **25**, 1815.
20 B. Maliszewska-Kordybach, *Appl. Geochem.*, 1996, **11**, 121–127.
21 P. Gao, E. da Silva, L. Hou, N. Denslow and P. Xiang, *Environ. Int.*, 2018, **119**, 466–477.
22 H. Zheng, C. Qu, J. Zhang, S. A. Talpur, Y. Ding, X. Xing and S. Qi, *Environ. Geochem. Health*, 2019, **41**, 907–919.
23 N. Li, Y. Mu, Z. Liu, Y. Deng, Y. Guo, X. Zhang, X. Li, P. Yu, Y. Wang and J. Zhu, *Sci. Rep.*, 2018, **8**, 3075.
24 D. A. Sarigiannis, S. P. Karakitsios, D. Zikopoulos, S. Nikolaki and M. Kermenidou, *Environ. Res.*, 2015, **137**, 147–156.
25 C. Peng, Y. He, K. Zhang, Y. Zhang, X. Wan, M. Wang and W. Chen, *J. Environ. Manage.*, 2022, **319**, 115699.
26 R. Li, M. Cheng, Y. Cui, Q. He, X. Guo, L. Chen and X. Wang, *Int. J. Environ. Res. Public Health*, 2020, **17**, 6319.
27 P. Zhang and Y. Chen, *Sci. Total Environ.*, 2017, **605–606**, 1011–1020.
28 W. Yang, Y. Lang and G. Li, *Chemosphere*, 2014, **112**, 289–295.
29 Q. Wang, X. Xu, X. Cong, Z. Zeng, L. Xu and X. Huo, *Environ. Geochem. Health*, 2019, **41**, 191–210.
30 Y. Liu, P. Gao, J. Su, E. B. da Silva, L. M. de Oliveira, T. Townsend, P. Xiang and L. Q. Ma, *Chemosphere*, 2019, **214**, 220–227.
31 S. Kuppusamy, P. Thavamani, K. Venkateswarlu, Y. B. Lee, R. Naidu and M. Megharaj, *Chemosphere*, 2017, **168**, 944–968.
32 P. Qi, C. Qu, S. Albanese, A. Lima, D. Cicchella, D. Hope, R. Cerino, A. Pizzolante, H. Zheng, J. Li and B. De Vivo, *J. Hazard. Mater.*, 2019, **383**, 121158.
33 IAMAT, *Air Pollution*, Sierra Leone.
34 C. Qu, S. Albanese, W. Chen, A. Lima, A. L. Doherty, A. Piccolo, M. Arienzo, S. Qi and B. De Vivo, *Environ. Pollut.*, 2016, **216**, 500–511.
35 E. T. Taylor and S. Nakai, *Afr. J. Environ. Sci. Technol.*, 2012, **6**, 283–292.
36 E. T. Taylor, M. J. Wirmvem, V. H. Sawyerr and S. Nakai, *J. Environ. Anal. Toxicol.*, 2015, **5**, 307.
37 A. S. Mansaray, A.-B. M. Senior, I. J. Samai and B. M. Koroma, *Nat. Resour.*, 2015, **06**, 491–501.
38 A. Maïga, A. Amouzou, M. Bagayoko, C. M. Faye, S. S. Jiwani, D. Kamara, I. B. Koroma and O. Sankoh, *BMC Health Serv. Res.*, 2021, **21**, 1–12.
39 Y. Zheng, X. Luo, W. Zhang, B. Wu, F. Han, Z. Lin and X. Wang, *Environ. Pollut.*, 2012, **171**, 85–92.
40 C. Qu, X. Xing, S. Albanese, A. Doherty, H. Huang, A. Lima, S. Qi and B. De Vivo, *Atmos. Environ.*, 2015, **122**, 31–40.
41 X. Xing, Y. Zhang, D. Yang, J. Zhang, W. Chen, C. Wu, H. Liu and S. Qi, *Atmos. Environ.*, 2016, **139**, 131–138.

42 W. Chen, B. Peng, H. Huang, Y. Kuang, Z. Qian, W. Zhu, W. Liu, Y. Zhang, Y. Liao, X. Zhao, H. Zhou and S. Qi, *Int. J. Environ. Res. Public Health*, 2022, **19**(1), 263.
43 M. Pansu and J. Gautheyrou, Water Content and Loss on Ignition, *Handbook of Soil Analysis: Mineralogical, Organic and Inorganic Methods*, Springer Berlin Heidelberg, Berlin, Heidelberg, Germany, 2006, pp. 3–13.
44 I. C. T. Nisbet and P. K. LaGoy, *Regul. Toxicol. Pharmacol.*, 1992, **16**, 290–300.
45 IARC, *IARC Monogr. Eval. Carcinog. Risks Hum.*, 1983, **32**, 211–224.
46 M. Nadal, M. Schuhmacher and J. L. Domingo, *Chemosphere*, 2007, **66**, 267–276.
47 J. Liu, G. Liu, J. Zhang, H. Yin and R. Wang, *J. Environ. Monit.*, 2012, **14**, 2634–2642.
48 M. Thiombane, S. Albanese, M. Di Bonito, A. Lima, D. Zuzolo, R. Rolandi, S. Qi and B. De Vivo, *Environ. Geochem. Health*, 2019, **41**, 507–528.
49 Q. Luo, L. Gu, Y. Shan, H. Wang and L. Sun, *Environ. Geochem. Health*, 2020, **42**, 1817–1832.
50 T. Agarwal, P. S. Khillare, V. Shridhar and S. Ray, *J. Hazard. Mater.*, 2009, **163**, 1033–1039.
51 H. B. Zhang, Y. M. Luo, M. H. Wong, Q. G. Zhao and G. L. Zhang, *Distributions and Concentrations of PAHs in Hong Kong Soils*, 2006, vol. 141.
52 N. Bortey-Sam, Y. Ikenaka, S. M. M. Nakayama, O. Akoto, Y. B. Yohannes, E. Baidoo, H. Mizukawa and M. Ishizuka, *Sci. Total Environ.*, 2014, **496**, 471–478.
53 B. Williams, J. Beah, E. Taylor, T. Kamara and D. Kaitibi, *Atmos. Clim. Sci.*, 2016, **7**, 1–10.
54 T. Agarwal, P. Khillare, V. Shridhar and S. Ray, *J. Hazard. Mater.*, 2009, 1033–1039.
55 CARPHA, *National Implementation Plan (NIP) for the Stockholm Convention on Persistent Organic Pollutants (POPs) for Saint Kitts and Nevis*, 2018.
56 A. Jin, J. He, S. Chen and G. Huang, *Environ. Sci.: Processes Impacts*, 2014, **16**, 1526–1534.
57 N. T. Edwards, *J. Environ. Qual.*, 1983, **12**, 427–441.
58 C. F. Munyeza, E. R. Rohwer and P. B. C. Forbes, *Trends Environ. Anal. Chem.*, 2019, **24**, e00070.
59 L. Pozzoli, S. Gilardoni, M. G. Perrone, G. De Gennaro, M. De Rienzo and D. Vione, *Ann. Chim.*, 2004, **94**, 17–33.
60 A. R. Johnsen, L. Y. Wick and H. Harms, *Environ. Pollut.*, 2005, **133**, 71–84.
61 L. Tolun, D. Martens, O. S. Okay and K. W. Schramm, *Environ. Int.*, 2006, **32**, 758–765.
62 M. Yunker, R. Macdonald, R. Vingarzan, R. Mitchell, D. Goyette and S. Strachan, *Org. Geochem.*, 2002, **33**, 489–515.
63 M. Tobiszewski and J. Namieśnik, *Environ. Pollut.*, 2012, **162**, 110–119.
64 X. Bi, W. Luo, J. Gao, L. Xu, J. Guo, Q. Zhang, K. Y. Romesh, J. P. Giesy, S. Kang and J. de Boer, *Sci. Total Environ.*, 2016, **556**, 12–22.
65 M. N. Islam, M. Park, Y.-T. Jo, X. P. Nguyen, S.-S. Park, S.-Y. Chung and J.-H. Park, *J. Geochem. Explor.*, 2017, **180**, 52–60.
66 D. Deyerling, J. Wang, W. Hu, B. Westrich, C. Peng, Y. Bi, B. Henkelmann and K.-W. Schramm, *Sci. Total Environ.*, 2014, **491–492**, 123–130.
67 J. Yang, Y. Yang, R.-S. Chen, X.-Z. Meng, J. Xu, A. Qadeer and M. Liu, *Environ. Pollut.*, 2017, **235**, 1–10.
68 R. Larsen and J. Baker, *Environ. Sci. Technol.*, 2003, **37**, 1873–1881.
69 Q. Zuo, Y. H. Duan, Y. Yang, X. J. Wang and S. Tao, *Environ. Pollut.*, 2007, **147**, 303–310.
70 S. S. Park, Y. J. Kim and C. H. Kang, *Atmos. Environ.*, 2002, **36**, 2917–2924.
71 X.-T. Wang, L. Chen, X.-K. Wang, B.-L. Lei, Y.-F. Sun, J. Zhou and M.-H. Wu, *Chemosphere*, 2015, **119**, 1224–1232.
72 J. Wang, J. Cao, Z. Dong, B. Guinot, M. Gao, R. Huang, Y. Han, Y. Huang, S. S. H. Ho and Z. Shen, *Environ. Pollut.*, 2017, **231**, 1330–1343.
73 W. Rogge, L. Hildemann, M. Mazurek, G. Cass and B. Simoneit, *Environ. Sci. Technol.*, 1993, **27**, 636–651.
74 Y.-H. Lang, G.-L. Li, X.-M. Wang, P. Peng and J. Bai, *Chemosphere*, 2015, **120**, 431–437.
75 H. Yuan, E. Liu, E. Zhang, W. Luo, L. Chen, C. Wang and Q. Lin, *Chemosphere*, 2017, **173**, 78–88.
76 X. Bi, W. Luo, J. Gao, L. Xu, J. Guo, Q. Zhang, K. Y. Romesh, J. P. Giesy, S. Kang and J. de Boer, *Sci. Total Environ.*, 2016, **556**, 12–22.
77 Y. Ellili-Bargaoui, C. Walter, B. Lemercier and D. Michot, *Ecol. Indic.*, 2021, **121**, 107211.
78 C. Degrendele, O. Audy, J. Hofman, J. Kucerik, P. Kukucka, M. D. Mulder, P. Přibylová, R. Prokeš, M. Sanka, G. E. Schaumann and G. Lammel, *Environ. Sci. Technol.*, 2016, **50**, 4278–4288.
79 Z. Lu, F. Zeng, N. Xue and F. Li, *Sci. Total Environ.*, 2012, **433**, 50–57.
80 M. Nadal, M. Schuhmacher and J. L. Domingo, *Environ. Pollut.*, 2004, **132**, 1–11.
81 M. N. Islam, M. Park, Y.-T. T. Jo, X. P. Nguyen, S.-S. S. Park, S.-Y. Y. Chung and J.-H. H. Park, *J. Geochem. Explor.*, 2017, **180**, 52–60.
82 T. Agarwal, P. S. Khillare and V. Shridhar, *Environ. Monit. Assess.*, 2007, **123**, 151–166.
83 J. Nam, G. Thomas, F. Jaward, E. Steinnes, O. Gustafsson and K. Jones, *Chemosphere*, 2008, **70**, 1596–1602.
84 B. Maliszewska-Kordybach, B. Smreczak and A. Klimkowicz-Pawlas, *Sci. Total Environ.*, 2009, **407**, 3746–3753.
85 J. Liu, Y. J. Liu, Z. Liu, A. Zhang and Y. Liu, *Environ. Geochem. Health*, 2019, **41**, 617–632.
86 I. Ololade, I. Arogunrerin, N. Oladoja, O. Ololade and A. Alabi, *Arch. Environ. Contam. Toxicol.*, 2021, **80**, 1–10.
87 A. Paschke, B. Vrana, P. Popp and G. Schüürmann, *Environ. Pollut.*, 2006, **144**, 414–422.
88 C. Qu, S. Albanese, A. Lima, J. Li, A. Doherty, S. Qi and B. De Vivo, *Environ. Pollut.*, 2017, **231**, 1497–1506.
89 E. Kalisa, S. Archer, E. Nagato, E. Bizuru, K. Lee, N. Tang, S. Pointing, K. Hayakawa and D. Lacap-Bugler, *Int. J. Environ. Res. Public Health*, 2019, **16**, 941.